Available online at www.sciencedirect.com

ScienceDirect

Underground Space 22 (2025) 355–368

www.keaipublishing.com/undsp

Research Paper

Wall movement during dewatering inside a diaphragm wall before soil excavation

Chao-Feng Zeng [a], William Powrie [b,*], Chang-Jie Xu [c], Xiu-Li Xue [a]

[a] *Hunan Provincial Key Laboratory of Geotechnical Engineering for Stability Control and Health Monitoring, School of Civil Engineering, Hunan University of Science and Technology, Xiangtan 411201, China*

[b] *Infrastructure Research Group, Faculty of Engineering and Physical Sciences, University of Southampton, Southampton SO17 1BJ, UK*

[c] *State Key Laboratory of Performance Monitoring Protecting of Rail Transit Infrastructure, East China Jiaotong University, Nanchang 330013, China*

Received 27 July 2024; received in revised form 3 January 2025; accepted 17 January 2025
Available online 3 April 2025

Abstract

Significant movement of in-situ retaining walls is usually assumed to begin with bulk excavation. However, an increasing number of case studies show that lowering the pore water pressures inside a diaphragm wall-type basement enclosure prior to bulk excavation can cause wall movements in the order of some centimeters. This paper describes the results of a laboratory-scale experiment carried out to explore mechanisms of in situ retaining wall movement associated with dewatering inside the enclosure prior to bulk excavation. Dewatering reduces the pore water pressures inside the enclosure more than outside, resulting in the wall moving as an unpropped cantilever supported only by the soil. Lateral effective stresses in the shallow soil behind the wall are reduced, while lateral effective stresses in front of the wall increase. Although the associated lateral movement was small in the laboratory experiment, the movement could be proportionately larger in the field with a less stiff soil and a potentially greater dewatered depth. The implementation of a staged dewatering system, coupled with the potential for phased excavation and propping strategies, can effectively mitigate dewatering-induced wall and soil movements. This approach allows for enhanced stiffness of the wall support system, which can be dynamically adjusted based on real-time displacement monitoring data when necessary.

Keywords: Deep excavation; Dewatering; Diaphragm wall deflection; Groundwater control; Laboratory experiment

1 Introduction

An increasing proportion of the world's increasing population lives in cities. Rapid urbanization has led to a need to develop underground space, often involving the construction of deep basements close to existing buildings and infrastructure. Interactions between new and existing constructions have long been a focus of research, with a key concern being to understand the effect of a new excavation on the surrounding built environment (Powrie & Li, 1991; Powrie & Chandler, 1998; Richards & Powrie, 1998; Ou et al., 2000; Hashash & Whittle, 2002; Powrie & Daly, 2007; Whittle et al., 2015; Faustin et al., 2018; Zhang et al., 2018b; Finno et al., 2019; Sailer et al., 2019; Zhang et al., 2021; Pujades & Jurado, 2021; Ong et al., 2022; Xue et al., 2022, 2023, 2024; Yang et al., 2025; Zeng et al., 2022a, 2023, 2024, 2022b; Ong & Chong, 2023; Ge et al., 2024; Qiao et al., 2024).

The stages of deep basement construction may be categorized into two groups (Zeng et al., 2018). The first group comprises the construction of the enclosure structure (e.g., a diaphragm or pile wall) and lowering the groundwater level by dewatering. These two stages are normally carried out in advance of bulk excavation and may include a check on whether the dewatering system (installed wells and pumping capacity) will satisfy the design drawdown requirements (Preene & Powrie, 1993; Powrie & Preene, 1994; Powrie & Roberts, 1995; Knight et al., 1996; Roy

* Corresponding author.
E-mail address: wp@soton.ac.uk (W. Powrie).
Peer review under the responsibility of Tongji University

https://doi.org/10.1016/j.undsp.2025.01.003
2467-9674/

Nomenclature

A_{ss}	soil loss area due to ground surface settlement	k_h	permeability in horizontal direction
A_w	soil loss area due to wall deflection	k_v	permeability in vertical direction
C	coefficient in Sichardt's formula to compute distance of influence	L_0	distance of influence
C_c	coefficient of curvature	n	actual porosity of soil
C_u	coefficient of uniformity	S	storage coefficient
e	void ratio of soil	t	the time taken to achieve the steady drawdown
$E'_{o0.1-0.2}$	constrained modulus	ω	water content
H	groundwater drawdown	ρ	soil density
H_e	final excavation depth	ρ_s	grain density
k	soil permeability		

& Robinson, 2009; Bevan et al., 2010; Pujades et al., 2014; Wu et al., 2019; Zheng et al., 2019a, 2019b; Ha et al., 2020; Xie et al., 2021; Zeng et al., 2019c, 2021a, 2021b, 2021c, 2021d, 2022c; Yang et al., 2023; He et al., 2024; Sun et al., 2024). The second group of basement construction activities comprises some or all staged excavation (possibly following further, staged dewatering), slab (or strut) construction, removal of struts and backfilling, and recovery of the groundwater level; all of these are carried out during or after bulk excavation.

Considerable attention has been paid to retaining wall and soil deformations, as well as aspects of structural behaviour such as strut loads associated with the second group of processes (Burland et al., 1977; Potts & Fourie, 1986; Bolton & Powrie, 1987, 1988; Clough & O'Rourke, 1990; Bolton & Stewart, 1994; Hashash & Whittle, 1996; Powrie, 1996; Richards et al., 1999; Batten & Powrie, 2000; Powrie & Batten, 2000; Finno & Calvello, 2005; Zdravkovic et al., 2005; Schwamb et al., 2014; Finno et al., 2015; Orazalin et al., 2015; Whittle et al., 2015; Korff et al., 2016; Schwamb et al., 2016; Hsieh & Ou, 2018; Zhang et al., 2018a). Some investigations have been carried out into the effects of retaining wall installation (Ng et al., 1995; Powrie & Kantartzi, 1996; Gourvenec & Powrie, 1999; Richards et al., 2006, 2007; Choy et al., 2007; Comodromos et al., 2013; Liu et al., 2018). In contrast, only limited investigations have been carried out into the behaviour of an enclosure structure during dewatering before bulk excavation. Movements during this stage are generally neglected and are rarely monitored. However, if the enclosure structure has already been installed prior to dewatering, it will be subjected to potentially significant changes in lateral pressure associated with dewatering and may move as a result.

Field observations during a dewatering test in soft soils (mainly silty clays and silts) in Tianjin, China reported by Zheng et al. (2014) and Zeng et al. (2019b) showed that dewatering before bulk soil excavation caused deflections of the enclosure structure and settlement of the surrounding ground up to 15 mm. Numerical simulations (Zeng et al., 2018, 2019b) of dewatering prior to excavation showed that the deformation of the enclosure during dewatering would vary with soil permeability and compressibility, the excavation geometry and the dewatered depth. The analyses indicated that significant retaining wall deflections may appear much earlier than often thought (i.e., before bulk excavation); monitoring and analysis that does not take this into account may underestimate the effect of basement excavation on the surrounding built environment.

The neglect of ground and retaining wall movements during pre-excavation dewatering means that there is a lack of experimental data to quantify the problem, or enable verification of numerical analyses. Although there are some scaling issues, simplified physical models tested in the laboratory can provide at least a qualitative understanding of the mechanism of dewatering-induced enclosure and soil deformation before excavation.

Laboratory-scale experiments have also been used to quantify certain aspects of groundwater flow associated with basement dewatering, e.g., the effects of partial flow blockage by a contiguous pile retaining wall (Richards et al., 2016), the blocking effect of enclosure structures on groundwater flow (Xu et al., 2014), and the response of the soil to groundwater abstraction (Li et al., 2014; Wang et al., 2018b). In these studies, the dewatering wells were not modelled explicitly; rather, the water level was regulated by means of a series of drainage holes in the side of the test chamber. Wang et al. (2018a) and Xu et al. (2019) used individual miniature wellpoints in a laboratory investigation of the drawdown vs. distance curves achieved by wells of different length. However, they did not investigate the potential for dewatering-induced movement of a retaining wall if groundwater lowering inside the wall is carried out in advance of excavation. To the best of our knowledge, this problem has not yet been investigated through laboratory-scale experiments and the mechanism of dewatering-induced enclosure movement before excavation is still not adequately understood.

This paper reports the results of a laboratory-scale experiment carried out to simulate dewatering before excavation of the soil in front of a diaphragm-type retaining wall. The full-scale geometry was reduced by a scale factor of 50, and miniature wellpoints were used to achieve the target groundwater level reduction. During the test, the water level changes inside and outside the basement diaphragm wall, the lateral movement of the enclosure structure, the ground settlement outside the excavation, and the lateral total and pore water pressures on both sides of the retaining wall were monitored. The experimental results are compared qualitatively with computations by others, and the mechanisms of dewatering-induced deflections of the retaining wall and the surrounding ground are discussed.

2 Laboratory-scale experiment

2.1 Engineering background

The laboratory experiment was based on a deep excavation for the Tianjin Metro Line 3, approximately 20 m wide and 17.4 to 19.1 m deep (Fig. 1). The basement enclosure was constructed from a series of diaphragm wall segments, with a depth of 33 m and thickness of 0.8 m. The excavation was divided into two sections: "Pit A" to the east and "Pit B" to the west.

The soil at the site comprised mainly silty clays, silts and silty fine sands to a depth of 42 m below original ground level (BGL). The initial groundwater level was at approximately 0.8 m BGL. To protect an existing, old three-story brick building on shallow foundations located at a distance of 8 m from the south of Pit B, the allowable lateral movement of the diaphragm wall was limited to a maximum of 0.14%H_e (i.e., about 27 mm), where H_e is the final excavation depth. This project is described in detail by Zheng et al. (2014).

To assess the performance of the groundwater control system, dewatering was carried out in Pit A for 10 days before bulk excavation of the soil from the enclosure com-

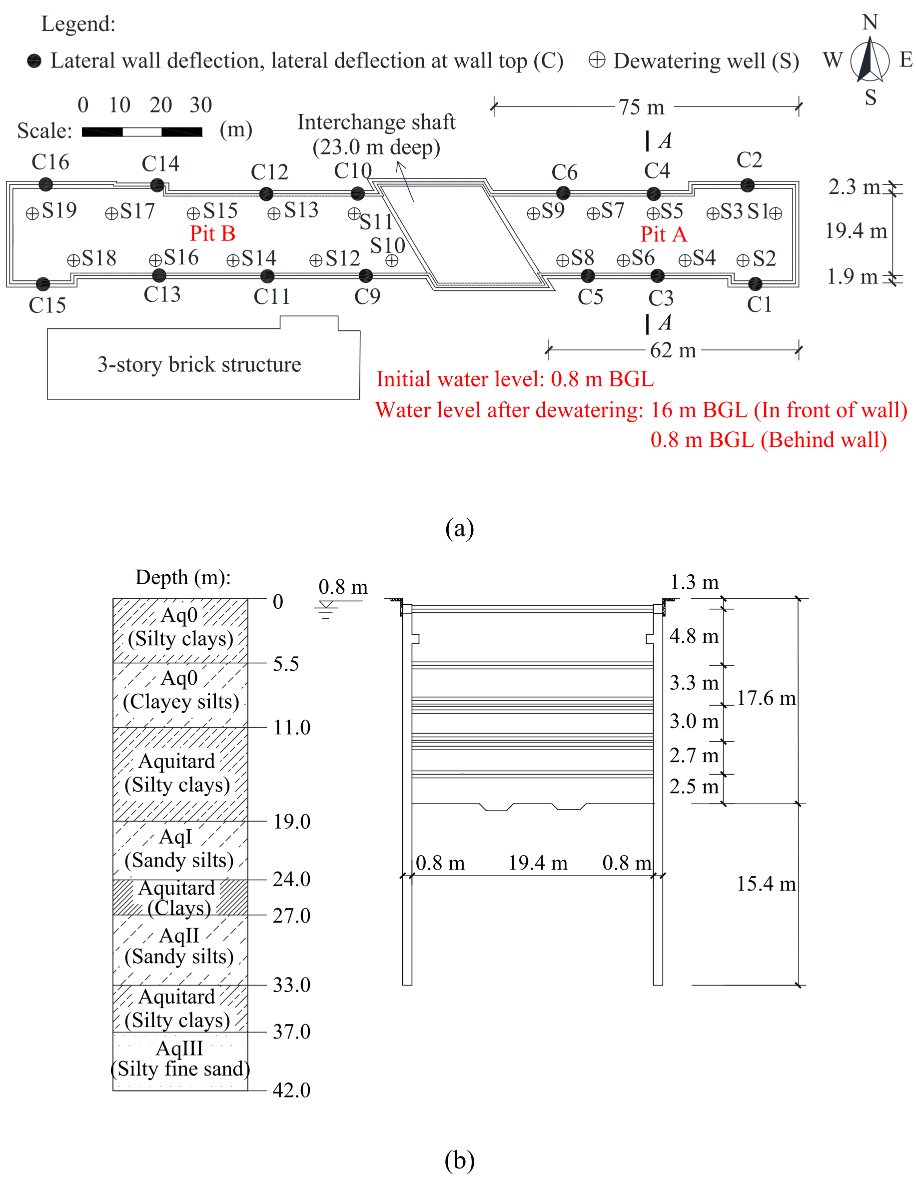

Fig. 1. (a) Plan view, and (b) cross section at A-A of deep excavation in Tianjin forming the basis of the experimental study reported in this paper. (adapted from Zheng et al. (2014))

menced. During this period, the dewatering pumps were placed sequentially at depths of 4, 8, 12, and then 16 m BGL, with dewatering continuing for 2.5 days at each depth. At each stage, the water level inside the wells and the excavation reached the required depth, but outside the diaphragm wall enclosure it remained unchanged.

All of the inclinometers embedded within the diaphragm wall enclosing Pit A showed inward horizontal displacement. The maximum displacement was approximately 10 mm at location C3 (Fig. 2). This represented 37.6% of the total allowable enclosure displacement. Limiting the deformation due to the subsequent construction process to the remaining 62.4% of the allowable displacement was considered too great a challenge; hence, jet grouting was used to stiffen and strengthen the soil to a depth of approximately 10 m below the final excavation floor. This was not part of the original design, incurred additional cost and delay, and ultimately was not fully successful in that the deflections of the diaphragm wall still exceeded the allowable value.

This case study shows that, where deformations around a new excavation are important, the movement of the enclosure during groundwater lowering prior to excavation should be considered. Reliable estimation would enable designers to plan the works differently, e.g., by specifying a stiffer retaining wall or more levels of propping during excavation. It might also be possible to optimize the sequence of dewatering, excavation, and propping so as to minimize overall wall displacements, including those during dewatering. However, selection of suitable methods of calculation and mitigation requires knowledge of the underlying mechanism(s) of soil/structure interaction during the dewatering stage. This cannot be obtained from the case study, as only the wall movements and lowered groundwater levels were recorded; and as mentioned earlier, a numerical model requires validation. The aim of the laboratory experiment reported in this paper was to determine the pattern of wall deflection, settlement of the surrounding ground surface, and the changes in total lateral earth and pore water pressures on both sides of the wall in response to a change in the groundwater level inside the excavation.

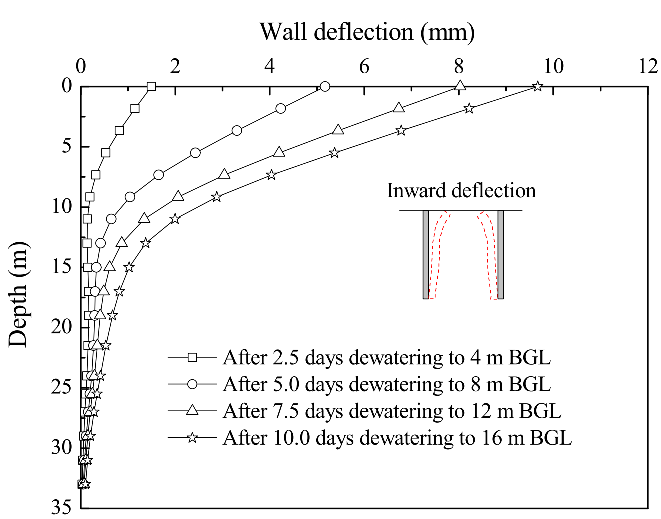

Fig. 2. Enclosure deflection at C3. (adapted from Zheng et al. (2014))

2.2 Experiment design

The geometry of the experiment was based on that of the excavation in Tianjin shown in Fig. 1. As the main objective was to provide insights into the generic mechanisms of diaphragm wall behaviour during dewatering, it was not attempted to replicate the soil types and layering with appropriately scaled soil strength, stiffness, and hydraulic conductivity, or the details of the actual dewatering process on site.

The experiment was carried out at a geometric scale of 1:50. Figure 3 shows the relationship between the actual dewatered area and the experiment, which modelled a short section towards the middle of the long and narrow real basement pit assuming conditions of plane flow and strain. Using symmetry, only half of the basement width was modelled in the experiment.

2.3 Test chamber

The test chamber, shown in Figs. 3 and 4, was 2.0 m long, 0.5 m wide and 1.0 m high. 0.5 m portion of the 2.0 m length was occupied by a water tank, separated from the soil by a perforated plate to allow free flow of water. The water level in the tank was maintained constant at 4 cm below the level of the soil surface, simulating a recharge boundary at a distance of 65 m from the edge (75 m from the centerline) of the real excavation. The test chamber was constructed from steel plate, except for the Perspex front wall that allowed observation of soil and diaphragm wall movements during testing. Stiffeners attached to the outer sides of the test chamber increased its rigidity to minimize out-of-plane deflections. Lubricated plastic films on the inner sides of the soil box, following Powrie and Daly (2007), reduced the side friction coefficient to about 0.1 times the effective friction angle of the soil.

The experiment was carried out in a uniform medium sand of measured permeability k ranging from 1.53×10^{-4} to 2.55×10^{-4} m/s (Table 1). For a drawdown $H = 0.26$ m as expected in the experiment, Sichardt's empirical formula,

$$L_0 = C \cdot H \cdot \sqrt{k} \tag{1}$$

yielded an influence distance L_0 of 4.82–6.23 m, taking $C = 1500\ (\text{m/s})^{-1/2}$ for plane flow. This is rather larger than the distance to the recharge boundary of 1.3 m in the test chamber. However, the diaphragm wall enclosure reduces the influence distance of an individual well (Bevan et al., 2010), and the 1.3 m influence distance matches that experimentally determined by Xu et al. (2019) in a laboratory-scale model dewatering experiment with similar soil and excavation geometry.

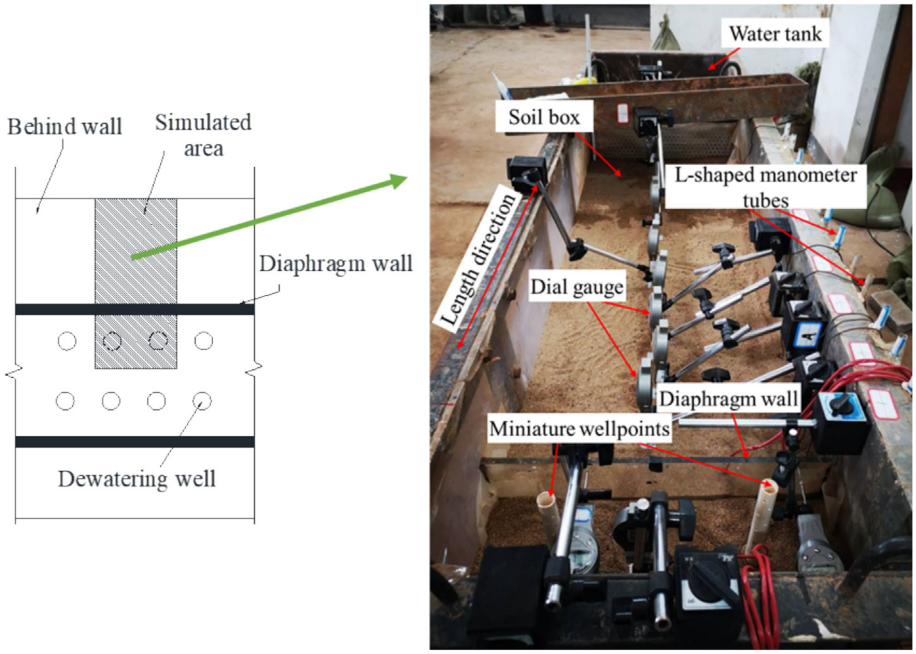

Fig. 3. Area simulated in the experiment and the model test chamber.

2.4 Dewatering and monitoring systems

Figure 4 shows the layout of the miniature wellpoints used to lower the groundwater level inside the model diaphragm wall enclosure and the monitoring points at which pore water pressure, total lateral pressures, and wall/soil movements were measured.

The miniature wellpoints were formed from 20 mm dia. PVC pipe, with ~4 mm dia. holes drilled in it to give an open area ratio of about 8%, which is within the range of 4%–20% for typical real wellscreens (Yao et al., 2006). The buried sections of the miniature wellpoints were wrapped in gauze to prevent the pumping of soil grains. Water was removed from the miniature wellpoints using a suction pump, although no vacuum was applied to the soil.

Clear Perspex L-shaped manometer tubes (labelled T1–T20), 10 mm in diameter, were used to manually observe pore water pressure heads along the base of the soil box. The horizontal sections were inserted into the sand at the bottom of the soil box, and the vertical sections were mounted on the sidewall (Fig. 4(b)). Scales on the vertical sections of the manometer tubes enabled direct measurement of changes in piezometric level at each of the monitoring points.

Total and pore water pressure transducers (DMT50 and DMK50) were mounted on both sides of the model diaphragm wall to monitor changes in total stress and pore water pressure during the experiment. Digital dial gauges with a resolution of 0.01 mm (GuangLu312-103-10) were used to manually record the settlement of the ground surface and the horizontal displacement at the top of the model diaphragm wall. Wall deflections were also monitored by digital image analysis of photographs captured using a digital camera (Canon EOS 5D Mark IV) to obtain the deflection of the wall at different depths.

2.5 Model soil and diaphragm wall

As mentioned above, the main objective of the experiment was to investigate the mechanism, rather than to make an accurate prediction, of dewatering-induced diaphragm wall and soil deformations. Hence, the complicated multi-layered soils present at the Tianjin site were not reproduced in the experiment, which was carried out in what may be described, according to the Unified Soil Classification System (USCS) on the basis of its grading curve (Fig. 5), as coarse sand (SW). Grading and other parameters are summarized in Table 1. All the parameters were obtained using appropriate conventional test methods, as indicated in Table 1.

The model diaphragm wall was constructed of Perspex plate, 9 mm thick, with a Young's Modulus of 3.37 GPa measured in uniaxial compression. Its bending stiffness EI roughly satisfied scaling requirements in being 50^3 times less per linear metre in the model than in the real structure (800 mm in thickness with a Young's Modulus of 30 GPa). The buried depth of the Perspex plate was 660 mm, representing 33 m in reality. In order to avoid the groundwater behind the diaphragm wall flowing into the foundation pit inside through the side edges of the wall, plastic films were stuck on both the diaphragm wall and the test chamber, as shown in Fig. 6. The plastic films were folded and a small amount of displacement was reserved to facilitate the free movement of the diaphragm wall.

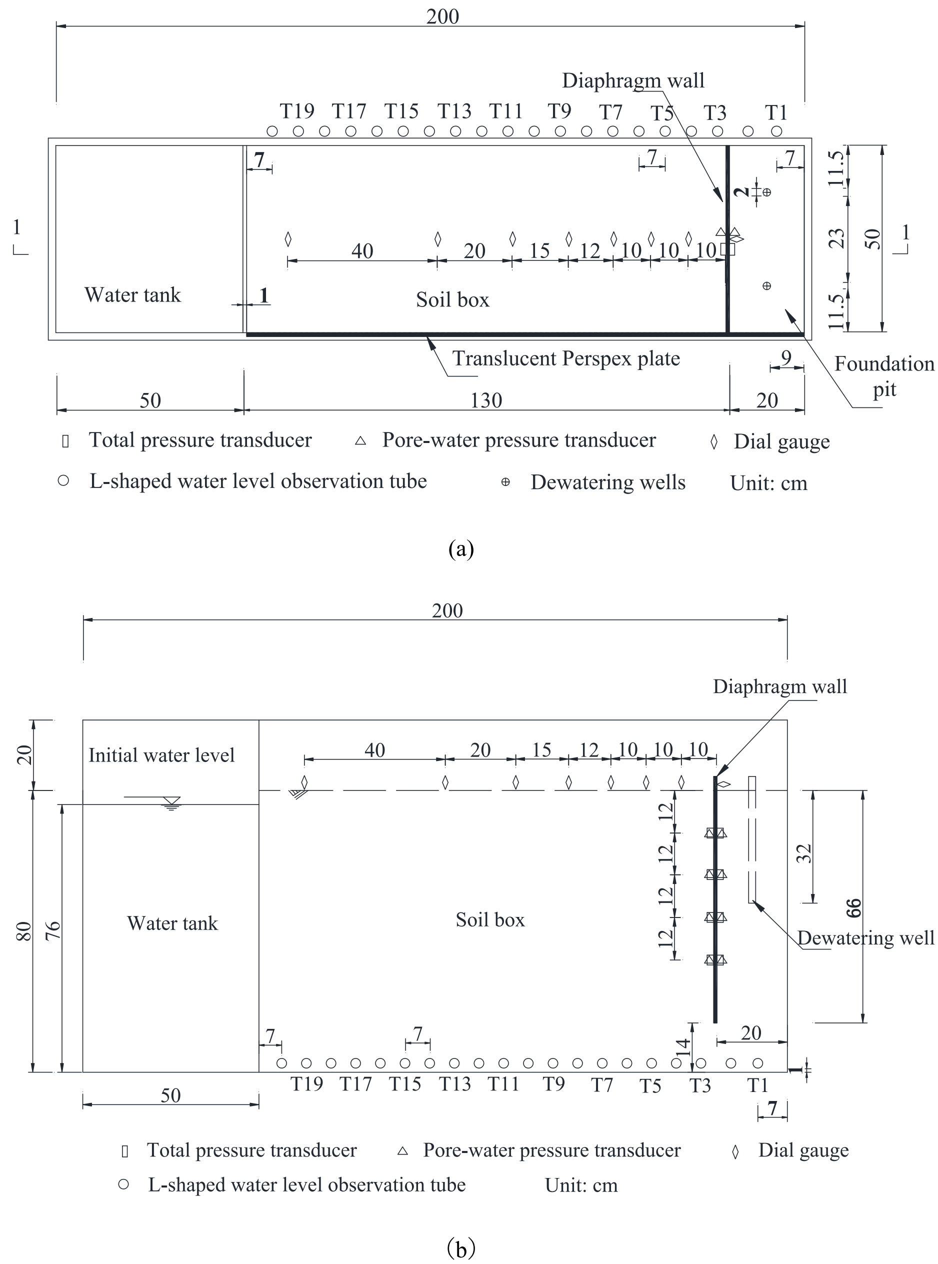

Fig. 4. Dewatering wells and monitoring points. (a) Plan layout, and (b) vertical section 1-1 (note: the excavation process was not performed while only pre-excavation dewatering was simulated). (adapted from Zeng et al. (2021a)).

Table 1
Grading and other parameters of the soil used in the laboratory model (adapted from Zeng et al. (2021a)).

Parameter	Symbol	Test method	Value
Soil description	–	PSD	Coarse sand
Coefficient of uniformity	C_u	PSD	4.04
Coefficient of curvature	C_c	PSD	1.48
As placed soil density	ρ (Mg/m^3)	Cutting-ring method	2.07
As placed soil water content	ω (%)	Oven-drying method	31.3
As placed grain density	ρ_s (Mg/m^3)	Pycnometer method	2.67
As placed void ratio	e	–	0.69
Darcy permeability	k (m/s)	Constant head permeameter	1.53×10^{-4} to 2.55×10^{-4} (mean: 2.1×10^{-4} m/s)
Constrained modulus	$E'_{o0.1\text{-}0.2}$ (MPa)	Oedometer test over stress range 100–200 kPa	9.63

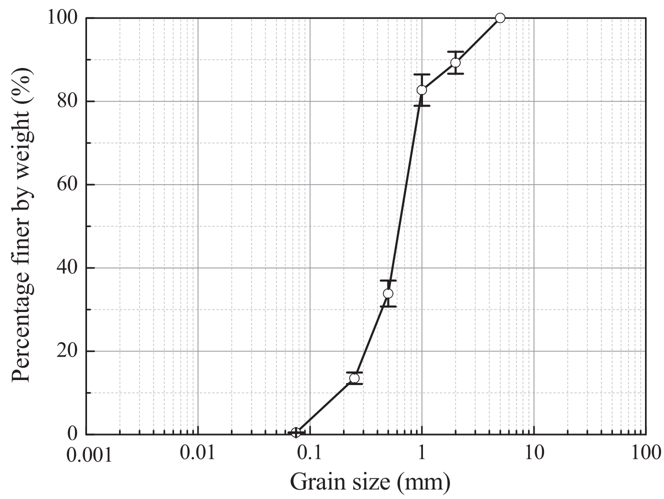

Fig. 5. Grading curve for the soil used in the model tests obtained by Zeng et al. (2021a).

2.6 Test procedure

The soil was placed and compacted into the box in layers, each 100 mm thick, up to the total depth of 800 mm. The weight of each layer was controlled during filling, and a small static penetrometer was used to confirm qualitatively the consistency of compaction. The dewatering wells, the model wall, and the total stress and pore water pressure transducers were installed during placement of the soil, followed by the dial gauges in the locations shown in Fig. 4.

Following placement, the soil was saturated by gradually raising the water level in the tank, slowly enough to maintain a near-horizontal level in the soil box, as observed in the manometer tubes. When the water level in the soil box was close to the soil surface (approximately 4 cm below the soil surface was observed), the water supply was turned off and the model was left to stand for a period of 24 h.

Before starting the experiment, the initial reading of each sensor was recorded. Pipes were then inserted into the two miniature wellpoints to a depth of 320 mm BGL (280 mm below the original groundwater level) and pumped using a suction pump. The water in the tank was kept at its initial level, and the readings of each sensor were recorded until a steady state was reached. Pumping then ceased and the water level was allowed to recover.

3 Experimental results and analyses

3.1 Pore water pressure head along the base of the soil box and water flowrate

Figure 7 shows the pore water pressure head along the base of the soil box at different times after the start of dewatering.

It took about 10 min for steady-state conditions to be achieved, after which the pore water pressure heads along the base of the box were essentially stable. This is consistent with the laboratory-scale dewatering experiment in a medium sand stratum with a similar well layout, as reported by Xu et al. (2019). According to Preene et al. (2016), for plane flow in an unconfined coarse-grained soil with permeability k greater than about 5×10^{-5} m/s, the time taken to achieve the steady-state drawdown (t) may be estimated as

$$t = \frac{8L_0^2 S}{27Hk}, \tag{2}$$

where S is the storage coefficient (defined as the volume of water released from the soil pores per unit area per unit drawdown), H is the drawdown, and L_0 is the distance of influence. For $L_0 = 1.3$ m, $H = 0.26$ m, k ranging from 1.53×10^{-4} to 2.55×10^{-4} m/s, and $t = 10$ min, Eq. (2) suggests a storage coefficient S in the range of 0.05–0.08. This is significantly smaller than (~12%–20% of) the actual

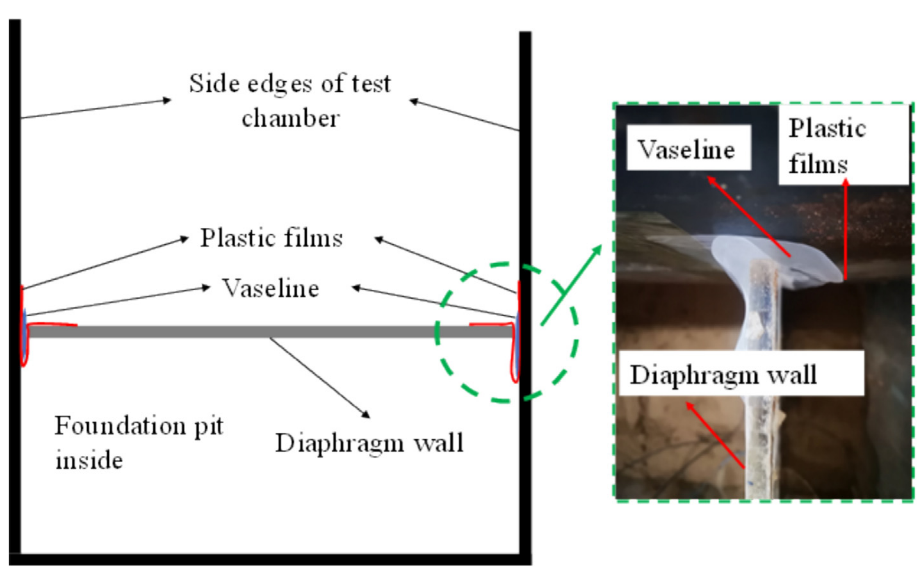

Fig. 6. Plastic films sticked on both diaphragm wall and test chamber to facilitate the free movement of diaphragm wall.

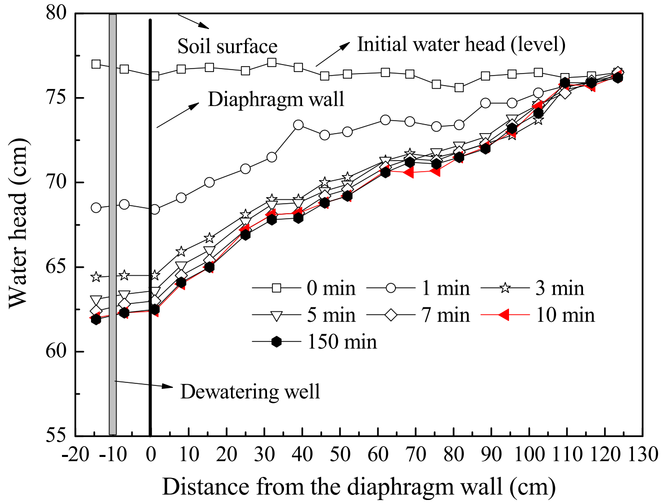

Fig. 7. Distribution of pore water pressure head along the base of the soil box at different times after the start of dewatering.

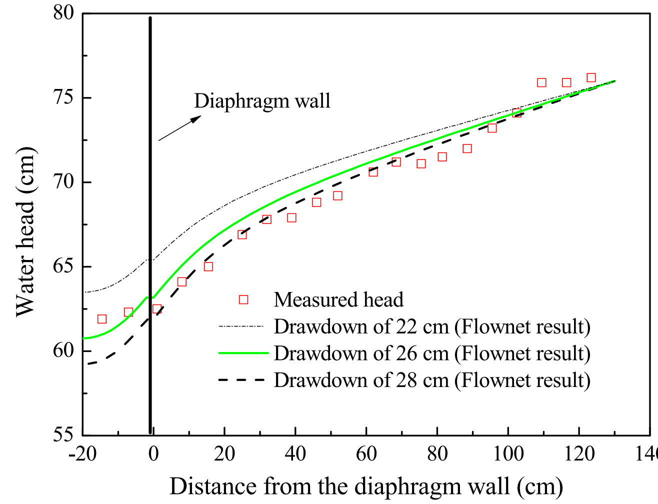

Fig. 8. Comparison of measured and calculated (flownet results) steady state heads along the base of the soil box.

porosity of the model soil ($n = e/(1+e) = 0.41$), but is consistent with the drainable porosity for a drawdown of about 0.3 m established in a laboratory draining cylinder test. However, this is an aspect of the model behaviour that would not scale quantitatively to field conditions.

Figure 8 compares the measured steady-state head along the base of the box with that calculated on the basis of a conventional plane flownet in a uniform soil, for effective water levels in front of the model diaphragm wall of 22, 26 and 28 cm below original groundwater level (i.e., 26, 30 and 32 cm below original ground level).

An effective drawdown inside the diaphragm wall of 26 cm gives the closest overall fit between the computed and measured water heads on both sides of the wall. The effective drawdown of 26 cm in front of the diaphragm wall for the purposes of the flow calculation may be compared with a steady-state water level inside the mini dewatering well of about 28 cm below original groundwater level, and the extrapolated location of the point of zero pore water pressure against the wall (Fig. 13) of approximately 16 cm below original groundwater level. These differences are due to the details of the flow pattern into the individual wells and head losses at entry into the well (Chenaf & Chapuis, 2007; Zeng et al., 2019a), which are neglected in the flownet calculation. Contours of equal head (equipotentials) for a drawdown of 26 cm inside the diaphragm wall, together with illustrative flowlines, are shown in Fig. 9.

Figure 10 shows the cumulative water yield and total discharge flow rate against time. The flow rate showed a slight decrease during the experiment to a steady value of about 5×10^{-4} m^3/min. The cumulative water yield increased approximately linearly, indicating that the variation in flow rate after the startup transient was small. Matching the flownet calculation (with 2 flowtubes, 10.4 head drops, an overall head drop of 0.26 m and a tank width of 0.5 m) to the measured steady-state flow rate implies an equivalent isotropic soil permeability of 3.33×10^{-4} m/s. Assuming a small degree of anisotropy such that $k_h = 4k_v$, gives a transformed section flownet with 2 flowtubes and 11 head drops and an implied equivalent permeability $\sqrt{(k_h k_v)} = 3.53 \times 10^{-4}$ m/s and a vertical permeability of 1.76×10^{-4} m/s, which is within the measured range of 1.53×10^{-4} to 2.55×10^{-4} m/s.

3.2 Enclosure deflection and ground surface settlement

Figure 11 shows the measured profiles of diaphragm wall deflection and soil surface settlement behind the wall at the end of the experiment. Upper and lower bounds to the observed soil surface settlement are shown, reflecting the limit of resolution of the digital dial gauges of 0.01 mm.

The wall deforms as a cantilever, consistent with the field observations described in Section 2.1. Within the limits of resolution of the digital dial gauges, the swept areas of the deflected shape (i.e., the volume loss or gain per unit length along the excavation) are similar (14.6 to 22.6 mm^3/mm soil surface settlement behind the wall, and 18.6 mm^3/mm deflection of the wall to the front). This suggests that the predominant mode of deformation is shear at constant volume owing to the movement of the retaining wall (Milligan & Bransby, 1976; Bolton & Powrie, 1987; Hsieh & Ou, 1998). Any consolidation settlement owing to the reduction in pore water pressure (increase in effective stress) is, as would be expected with a sand, relatively small.

The maximum settlement or wall deflection per unit drawdown in the experiment (0.06 to 0.07 mm per 260 mm, or 0.023% to 0.027%) is of the same order as the settlement of 3.4 mm for a drawdown of 16 m (0.021%) obtained by Zeng et al. (2018) in a numerical simulation of the project described in Section 2.1; although their calculated wall deflection (9.7 mm or 0.06% of the drawdown) was rather greater.

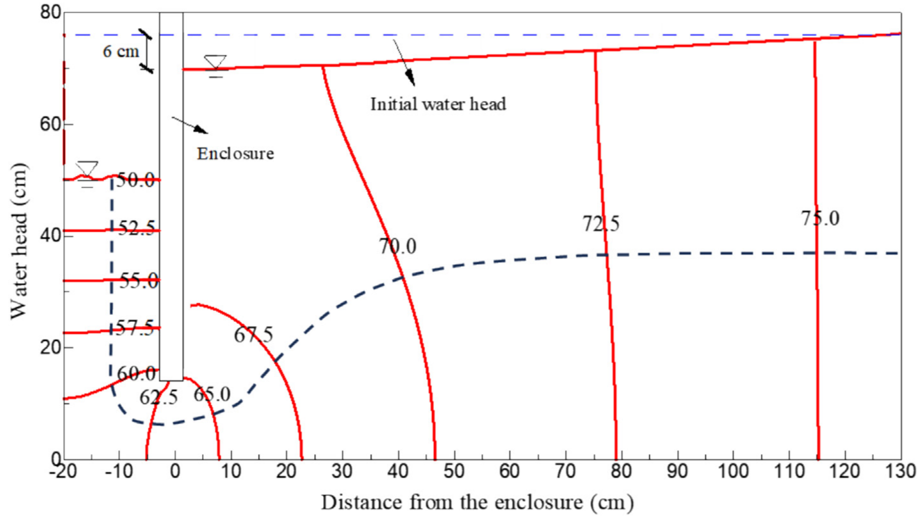

Fig. 9. Contour map of equal head (equipotentials) for a drawdown of 26 cm inside the diaphragm wall.

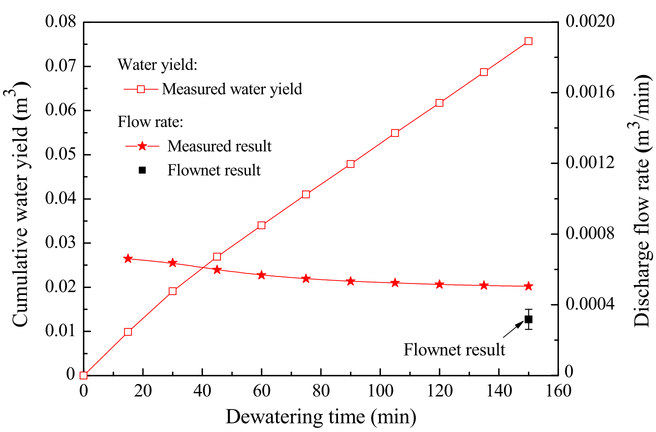

Fig. 10. Time history curves of cumulative water yield and discharge flow rate.

Figure 12 shows the maximum enclosure deflection, maximum surface settlement and the water head changes inside and outside the diaphragm wall measured during the experiment as functions of time.

Movements and drawdowns are broadly correlated, with rapid initial rates of change and reaching steady values within about 10 min. Multiplying by 50 to account for scale effects (assuming drainage by air entry rather than by consolidation), this would correspond to just over 8.3 h in the field for a soil of the same permeability (1.53×10^{-4} to 2.55×10^{-4} m/s). Even at full scale the wall and ground movements were small (i.e., about 3.5 mm). However, the dewatering depth in the experiment was limited (only 13 m at full scale); in a project with a greater dewatered depth and less stiff soil, wall and ground movements would be larger (Zeng et al., 2019b).

If it is necessary to restrict wall movements, for example to protect adjacent sensitive structures, a progressive switch-on of the dewatering combined with close monitoring of drawdowns and movements would enable dewatering to be paused should unexpectedly large movements occur. Consideration could then be given to staged dewatering, excavation and propping to increase the effective stiffness of the wall support during bulk excavation.

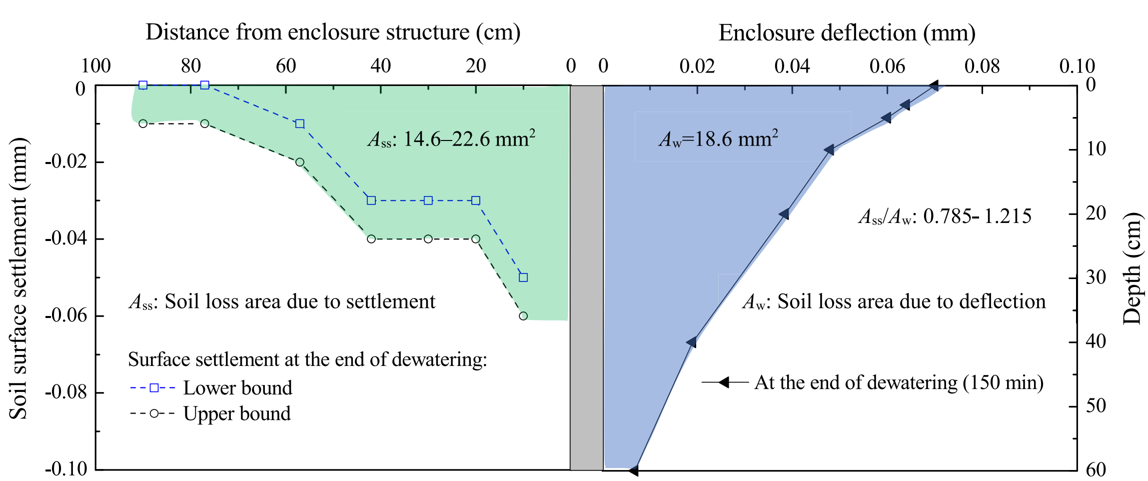

Fig. 11. Measured diaphragm wall deflection and soil surface settlement during experiment.

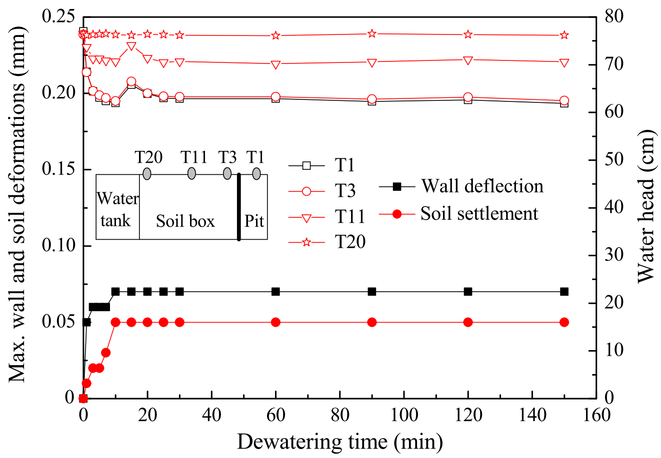

Fig. 12. Time histories of maximum wall deflection, maximum surface settlement and groundwater level changes inside and outside the diaphragm wall.

3.3 Changes in lateral total stress inside and outside the diaphragm wall

Figure 13 compares the distributions of pore water pressure measured on both sides of the wall with those calculated from the flownet. Error bars are based on variability noted during transducer calibration.

As would be expected (and is calculated from the flownet), there is a reduction in pore water pressure behind the wall owing to a reduction in the rate of increase in pore water pressure with depth, consistent with the development of downward seepage.

In front of the wall, there is a reduction in pore water pressure associated with a lowering of the effective groundwater level; the rate of increase of pore water pressure with depth increases, consistent with the development of upward seepage in this region. However, as has already been noted, the extrapolated depth of zero pore pressure on the wall inside the enclosure is approximately 16 cm below original groundwater level (i.e., 20 cm below original ground level), compared with an effective drawdown of 26 cm (i.e., 30 cm below original ground level) used in the flownet calculation and a drawdown of 28 cm measured in the miniature wellpoints.

Figure 14 shows the change in lateral total stress on both sides of the diaphragm wall at the end of the experiment, from an assumed initial condition (the initial lateral stress could not be measured reliably with the type of transducer used, owing to the disturbance of soil filling). Given the measured overall forward movement and rotation of the wall shown in Fig. 11, it is difficult to posit a rational physical explanation for the large reduction in lateral total stress measured in front of the wall at a depth of 35 cm below original ground level. It is assumed that this is due to a transducer malfunction, and is discounted from the remainder of the discussion.

Lowering the groundwater level inside the diaphragm wall led to a reduction in the total lateral stress on both sides of the wall. Discounting the assumed erroneous transducer reading, the reduction in lateral total stress was generally small except behind the wall over its upper 20 cm.

Figure 15 shows distributions of lateral effective stress behind and in front of the wall, calculated as the difference between the measured changes in total lateral stress and pore water pressure shown relative to the notional initial line.

Below 20 cm depth, ignoring the assumed erroneous data point, the lateral effective stresses increased on both sides of the wall. Above this depth, the lateral effective stresses outside the enclosure reduced, consistent with the observed pattern of wall movement. Dewatering-induced wall movement is to be triggered by a reduction in lateral total stress in front of the wall because of the reduction in pore pressure due to dewatering. As the wall then moves towards the enclosure in unpropped cantilever mode, equilibrium is restored by an increase in the lateral effective stresses in front and a reduction in the lateral effective stresses behind the wall, over its upper portion.

4 Conclusions

A laboratory-scale experiment was conducted to investigate wall and soil movements associated with dewatering around a diaphragm wall enclosure before excavation of the soil from inside. During the test, the water level changes behind and in front of the diaphragm wall, the lateral movement of the wall, the lateral stresses and pore water

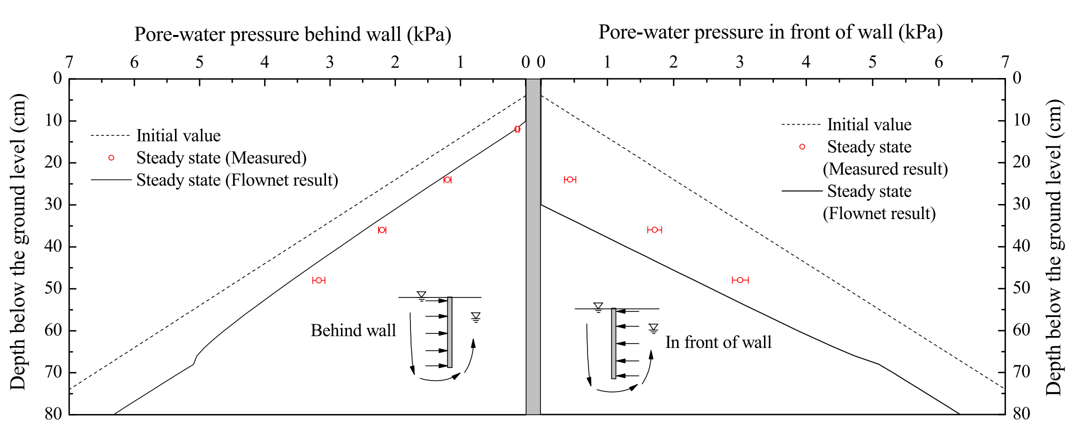

Fig. 13. Distributions of pore-water pressure on the wall outside and inside the excavation.

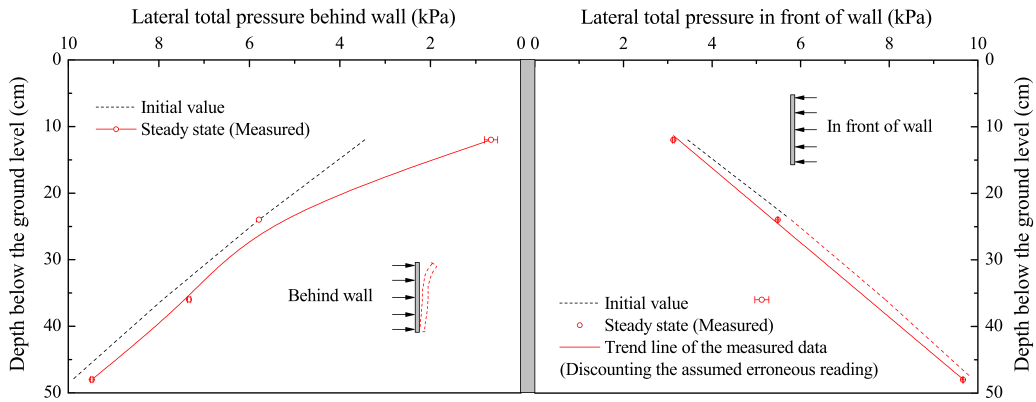

Fig. 14. Changes in lateral total stress behind and in front of the diaphragm wall.

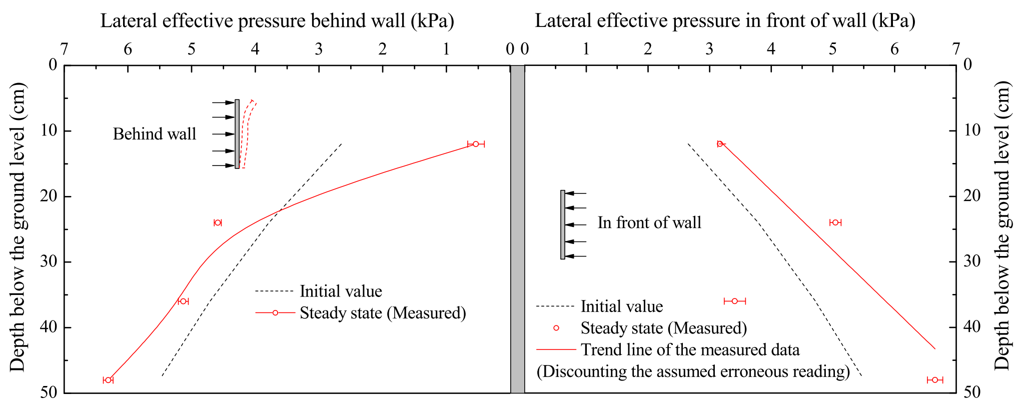

Fig. 15. Distributions of lateral effective stress on the wall outside and inside the excavation.

pressures on both sides of the wall and the settlement of the ground surface outside the wall were monitored. The measurements and their analysis have shown that:

(1) Scale modelling at normal gravity is able to reproduce broad mechanisms of groundwater level drawdown and wall movement, and the interactions between them. However, some details (for example, seepage face effects) do not scale, and the movements and changes in pressure that have to be measured are small.
(2) During the experiment, measurable wall movements were observed as the steady-state drawdown developed in response to pumping on miniature wellpoints, over a period of about 10 min. This is quite rapid, and suggests that—at the relatively low suction heads associated with the model—the drainable porosity of the soil at a drawdown of up to about 30 cm was only 10%–20% of the total. This is an aspect that would not scale directly to the field.
(3) Dewatering reduces the pore water pressure on both sides of the wall—particularly in front (inside the enclosure), where the drawdown in groundwater level is greatest. In response to these changes in pore pressure, the wall tends to move towards the excavation in unpropped cantilever mode. Equilibrium is maintained by an accompanying reduction in the lateral effective stresses behind the wall over its upper part and an increase in the lateral effective stresses in front.
(4) At this stage, the wall is supported only by the soil. Although in the laboratory experiment the associated lateral movement was small, in the field with a less stiff soil and a potentially greater dewatered depth, the movement could be proportionately larger. Dewatering-induced wall and soil movements could be reduced by commissioning the dewatering system in stages, with the option for staged excavation and propping to increase the stiffness of the wall support system should displacement monitoring indicate the need.

It should be noted that a generally qualitative study was performed through a laboratory-scale test in uniform sand soils; thus, the above qualitative results or conclusions could be kept for reference in the practical engineering while the quantitative results are not suggested to be used in practice. In the future, further tests in multi-layered soils could be performed to better reveal the response of diaphragm walls to excavation dewatering, based on which some quantitative equations may be obtained to evaluate the diaphragm wall behaviour.

Data availability

The data that support the findings of this study are available from the corresponding author upon reasonable request.

CRediT authorship contribution statement

Chao-Feng Zeng: Writing – original draft, Methodology. **William Powrie:** Writing – review & editing. **Chang-Jie Xu:** Investigation. **Xiu-Li Xue:** Formal analysis, Data curation.

Declaration of competing interest

The authors declare that they have no known competing financial interests or personal relationships that could have appeared to influence the work reported in this paper.

Acknowledgment

This work was supported by the National Natural Science Foundation of China (Grant Nos. 52478342 and 52238009), the Science and Technology Innovation Program of Hunan Province (Grant No. 2022RC1172), and the Natural Science Foundation of Jiangxi Province (Grant No. 20223BBG71018). Finally, we deeply appreciate the warm and efficient work of editors and reviewers.

References

Batten, M., & Powrie, W. (2000). Measurement and analysis of temporary prop loads at Canary Wharf underground station, east London. *Proceedings of the Institution of Civil Engineers - Geotechnical Engineering, 143*(3), 151–163.

Bevan, M. A., Powrie, W., & Roberts, T. O. L. (2010). Influence of large-scale inhomogeneities on a construction dewatering system in chalk. *Géotechnique, 60*(8), 635–649.

Bolton, M. D., & Powrie, W. (1987). The collapse of diaphragm walls retaining clay. *Géotechnique, 37*(3), 335–353.

Bolton, M. D., & Powrie, W. (1988). Behaviour of diaphragm walls in clay prior to collapse. *Géotechnique, 38*(2), 167–189.

Bolton, M. D., & Stewart, D. I. (1994). The effect on propped diaphragm walls of rising groundwater in stiff clay. *Géotechnique, 44*(1), 111–127.

Burland, J. B., Longworth, T. I., & Moore, J. F. A. (1977). A study of ground movement and progressive failure caused by a deep excavation in Oxford Clay. *Géotechnique, 27*(4), 557–591.

Chenaf, D., & Chapuis, R. P. (2007). Seepage face height, water table position, and well efficiency at steady state. *Groundwater, 45*(2), 168–177.

Choy, C. K., Standing, J. R., & Mair, R. J. (2007). Stability of a loaded pile adjacent to a slurry-supported trench. *Géotechnique, 57*(10), 807–819.

Clough, G. W., & O'Rourke, T. D. (1990). Construction induced movements of insitu walls. *Geotechnical Special Publication, 25*, 439–470.

Comodromos, E. M., Papadopoulou, M. C., & Konstantinidis, G. K. (2013). Effects from diaphragm wall installation to surrounding soil and adjacent buildings. *Computers and Geotechnics, 53*, 106–121.

Faustin, N. E., Elshafie, M. Z. E. B., & Mair, R. J. (2018). Case studies of circular shaft construction in London. *Proceedings of the Institution of Civil Engineers - Geotechnical Engineering, 171*(5), 391–404.

Finno, R. J., Arboleda-Monsalve, L. G., & Sarabia, F. (2015). Observed performance of the one museum park west excavation. *Journal of Geotechnical and Geoenvironmental Engineering, 141*(1), 04014078.

Finno, R. J., & Calvello, M. (2005). Supported excavations: observational method and inverse modeling. *Journal of Geotechnical and Geoenvironmental Engineering, 131*(7), 826–836.

Finno, R. J., Kim, S., Lewis, J., & Winkle, N. V. (2019). Observed performance of a sheetpile-supported excavation in Chicago clays. *Journal of Geotechnical and Geoenvironmental Engineering, 145*(2), 05018005.

Ge, C., Yang, M., Li, P., Zhang, M., & Zhang, Z. (2024). Performance and environmental impacts of deep foundation excavation in soft soils: a field and modeling-based case study in Nanjing, China. *Underground Space, 18*, 218–238.

Gourvenec, S. M., & Powrie, W. (1999). Three-dimensional finite-element analysis of diaphragm wall installation. *Géotechnique, 49*(6), 801–823.

Ha, D., Zheng, G., Zhou, H., Zeng, C., & Zhang, H. (2020). Estimation of hydraulic parameters from pumping tests in a multiaquifer system. *Underground Space, 5*(3), 210–222.

Hashash, Y. M. A., & Whittle, A. J. (1996). Ground movement prediction for deep excavations in soft clay. *Journal of Geotechnical Engineering, 122*(6), 474–486.

Hashash, Y. M. A., & Whittle, A. J. (2002). Mechanisms of load transfer and arching for braced excavations in clay. *Journal of Geotechnical and Geoenvironmental Engineering, 128*(3), 187–197.

He, D., Zeng, C., Xu, C., Xue, X., Zhao, Y., Han, L., & Sun, H. (2024). Barrier effect of existing building pile on the responses of groundwater and soil during foundation pit dewatering. *Water, 16*(20), 2977.

Hsieh, P. G., & Ou, C. Y. (1998). Shape of ground surface settlement profiles caused by excavation. *Canadian Geotechnical Journal, 35*(6), 1004–1017.

Hsieh, P. G., & Ou, C. Y. (2018). Mechanism of buttress walls in restraining the wall deflection caused by deep excavation. *Tunnelling and Underground Space Technology, 82*, 542–553.

Knight, D. J., Smith, G. L., & Sutton, J. S. (1996). Sizewell B foundation dewatering—system design, construction and performance monitoring. *Géotechnique, 46*(3), 473–490.

Korff, M., Mair, R. J., & Tol, F. A. F. V. (2016). Pile-soil interaction and settlement effects induced by deep excavations. *Journal of Geotechnical and Geoenvironmental Engineering, 142*(8), 04016034.

Li, Y., Hu, Z., Weng, T., Fonseca, J., & Zhang, X. (2014). Experimental study on the vertical deformation of sand caused by cyclic withdrawal and recharging of groundwater. *Engineering Geology, 183*, 247–253.

Liu, W., Shi, P., Li, H., & Wang, F. (2018). Observed performance of three adjacent 48 m depth concrete diaphragm wall panels in silty soils. *Canadian Geotechnical Journal, 56*(11), 1736–1742.

Milligan, G. W. E., & Bransby, P. L. (1976). Combined active and passive rotational failure of a retaining wall in sand. *Géotechnique, 26*(3), 473–494.

Ng, C. W., Lings, M. L., Simpson, B., & Nash, D. F. T. (1995). An approximate analysis of the three-dimensional effects of diaphragm wall installation. *Géotechnique, 45*(3), 497–507.

Ong, D. E. L., & Chong, E. E. M. (2023). Soil–structure interactions in a capped CBP wall system triggered by localized hydrogeological drawdown in a complex geological setting. *Geosciences, 13*(10), 304.

Ong, D. E. L., Jong, S. C., & Cheng, W. C. (2022). Ground and groundwater responses due to shaft excavation in organic soils. *Journal of Geotechnical and Geoenvironmental Engineering, 148*(8), 05022003.

Orazalin, Z. Y., Whittle, A. J., & Olsen, M. B. (2015). Three-dimensional analyses of excavation support system for the Stata Center basement on the MIT campus. *Journal of Geotechnical and Geoenvironmental Engineering, 141*(7), 05015001.

Ou, C. Y., Liao, J. T., & Cheng, W.-L. (2000). Building response and ground movements induced by a deep excavation. *Géotechnique, 50*(3), 209–220.

Potts, D. M., & Fourie, A. B. (1986). A numerical study of the effects of wall deformation on earth pressures. *International Journal for Numerical and Analytical Methods in Geomechanics, 10*(4), 383–405.

Powrie, W. (1996). Limit equilibrium analysis of embedded retaining walls. *Géotechnique, 46*(4), 709–723.

Powrie, W., & Batten, M. (2000). Comparison of measured and calculated temporary-prop loads at Canada Water Station. *Géotechnique, 50*(2), 127–140.

Powrie, W., & Chandler, R. J. (1998). The influence of a stabilizing platform on the performance of an embedded retaining wall: a finite element study. *Géotechnique, 48*(3), 403–409.

Powrie, W., & Daly, M. P. (2007). Centrifuge modelling of embedded retaining walls with stabilising bases. *Géotechnique, 57*(6), 485–497.

Powrie, W., & Kantartzi, C. (1996). Ground response during diaphragm wall installation in clay: centrifuge model tests. *Géotechnique, 46*(4), 725–739.
Powrie, W., & Li, E. S. F. (1991). Finite element analyses of an in situ wall propped at formation level. *Géotechnique, 41*(4), 499–514.
Powrie, W., & Preene, M. (1994). Time-drawdown behaviour of construction dewatering systems in fine soils. *Géotechnique, 44*(1), 83–100.
Powrie, W., & Roberts, T. O. L. (1995). Case history of a dewatering and recharge system in chalk. *Géotechnique, 45*(4), 599–609.
Preene, M., & Powrie, W. (1993). Steady-state performance of construction dewatering systems in fine soils. *Géotechnique, 43*(2), 191–205.
Preene, M., Roberts, T. O. L., & Powrie, W. (2016). *Groundwater control: Design and practice*. London: Construction Industry Research and Information Association.
Pujades, E., & Jurado, A. (2021). Groundwater-related aspects during the development of deep excavations below the water table: a short review. *Underground Space, 6*(1), 35–45.
Pujades, E., Vàzquez-Suñé, E., Carrera, J., & Jurado, A. (2014). Dewatering of a deep excavation undertaken in a layered soil. *Engineering Geology, 178*, 15–27.
Qiao, Y., Xie, F., Bai, Z., Lu, J., & Ding, W. (2024). Deformation characteristics of ultra-deep circular shaft in soft soil: a case study. *Underground Space, 16*, 239–260.
Richards, D. J., Clark, J., & Powrie, W. (2006). Installation effects of a bored pile wall in overconsolidated clay. *Géotechnique, 56*(6), 411–425.
Richards, D. J., Holmes, G., & Beadman, D. R. (1999). Measurement of temporary prop loads at Mayfair car park. *Proceedings of the Institution of Civil Engineers - Geotechnical Engineering, 137*(3), 165–174.
Richards, D. J., & Powrie, W. (1998). Centrifuge model tests on doubly propped embedded retaining walls in overconsolidated kaolin clay. *Géotechnique, 48*(6), 833–846.
Richards, D. J., Powrie, W., Roscoe, H., & Clark, J. (2007). Pore water pressure and horizontal stress changes measured during construction of a contiguous bored pile multi-propped retaining wall in Lower Cretaceous clays. *Géotechnique, 57*(2), 197–205.
Richards, D. J., Wiggan, C. A., & Powrie, W. (2016). Seepage and pore pressures around contiguous pile retaining walls. *Géotechnique, 66*(7), 523–532.
Roy, D., & Robinson, K. E. (2009). Surface settlements at a soft soil site due to bedrock dewatering. *Engineering Geology, 107*(3), 109–117.
Sailer, E., Taborda, D. M. G., Zdravković, L., & Potts, D. M. (2019). Fundamentals of the coupled thermo-hydro-mechanical behaviour of thermo-active retaining walls. *Computers and Geotechnics, 109*, 189–203.
Schwamb, T., Elshafie, M. Z. E. B., Soga, K., & Mair, R. J. (2016). Considerations for monitoring of deep circular excavations. *Proceedings of the Institution of Civil Engineers - Geotechnical Engineering, 169* (6), 477–493.
Schwamb, T., Soga, K., Mair, R. J., Elshafie, M. Z. E. B., Sutherden, R., Boquet, C., & Greenwood, J. (2014). Fibre optic monitoring of a deep circular excavation. *Proceedings of the Institution of Civil Engineers - Geotechnical Engineering, 167*(2), 144–154.
Sun, Y., Jiang, Z., Tong, L., Sun, J., Cui, J., Zhou, X., & Liu, S. (2024). Optimization of confined aquifer dewatering for long-deep excavation using simulation–optimization method. *Underground Space, 17*, 246–266.
Wang, J., Liu, X., Liu, S., Zhu, Y., Pan, W., & Jie, Z. (2018a). Physical model test of transparent soil on coupling effect of cut-off wall and pumping wells during foundation pit dewatering. *Acta Geotechnica*, 1–22.
Wang, J. X., Deng, Y. S., Ma, R. Q., Liu, X. T., Guo, Q. F., Liu, S. L., & Huang, X. L. (2018b). Model test on partial expansion in stratified subsidence during foundation pit dewatering. *Journal of Hydrology, 557*, 489–508.
Whittle, A. J., Corral, G., Jen, L. C., & Rawnsley, R. P. (2015). Prediction and performance of deep excavations for courthouse station, Boston. *Journal of Geotechnical and Geoenvironmental Engineering, 141*(4), 04014123.
Wu, Y.-X., Lyu, H.-M., Han, J., & Shen, S.-L. (2019). Dewatering-induced building settlement around a deep excavation in soft deposit in Tianjin, China. *Journal of Geotechnical and Geoenvironmental Engineering, 145*(5), 05019003.
Xie, Z.-F., Shen, S.-L., Arulrajah, A., & Horpibulsuk, S. (2021). Environmentally sustainable groundwater control during dewatering with barriers: a case study in Shanghai. *Underground Space, 6*(1), 12–23.
Xu, Y.-S., Yan, X.-X., Shen, S.-L., & Zhou, A.-N. (2019). Experimental investigation on the blocking of groundwater seepage from a waterproof curtain during pumped dewatering in an excavation. *Hydrogeology Journal, 27*, 2659–2672.
Xu, Y. S., Shen, S. L., Ma, L., Sun, W. J., & Yin, Z. Y. (2014). Evaluation of the blocking effect of retaining walls on groundwater seepage in aquifers with different insertion depths. *Engineering Geology, 183*, 254–264.
Xue, T., Xue, X., Long, S., Chen, Q., Lu, S., & Zeng, C. (2023). Effect of pre-existing underground structures on groundwater flow and strata movement induced by dewatering and excavation. *Water, 15*(4), 814.
Xue, X.-L., Sun, H.-Y., Zeng, C.-F., Chen, H.-B., Zheng, G., Xu, C.-J., & Han, L. (2024). Why pile-supported building settled continuously after water level was stabilized during dewatering: clues from interaction between pile and multi aquifers. *Journal of Hydrology, 638*, 131539.
Xue, X.-L., Zhu, L., Wang, S., Chen, H.-B., & Zeng, C.-F. (2022). *Groundwater Response to Pumping Considering Barrier Effect of Existing Underground Structure.* Paper presented at the Proceedings of the 4th International Conference on Performance Based Design in Earthquake Geotechnical Engineering, Cham.
Yang, K., Xu, C., Zeng, C., Zhu, L., Xue, X., & Han, L. (2025). Analysis of recharge efficiency under barrier effects incurred by adjacent underground structures. *Water, 17*(2), 257.
Yang, T., Tong, L.-Y., Hesham El Naggar, M., & Yan, X. (2023). Hydraulic head difference at two sides of suspended waterproof curtain during multi-grade dewatering of excavation. *Underground Space, 10*, 137–149.
Yao, T. Q., Shi, Z. H., & Cao, H. B. (2006). *Manual for foundation pit dewatering*. China Architecture and Building Press.
Zdravkovic, L., Potts, D. M., & John, H. D. S. (2005). Modelling of a 3D excavation in finite element analysis. *Géotechnique, 55*(7), 497–513.
Zeng, C.-F., Chen, H.-B., Liao, H., Xue, X.-L., Chen, Q.-N., & Diao, Y. (2023). Behaviours of groundwater and strata during dewatering of large-scale excavations with a nearby underground barrier. *Journal of Hydrology, 620*, 129400.
Zeng, C.-F., Liao, H., Xue, X.-L., Long, S.-C., Luo, G.-J., Diao, Y., & Li, M.-G. (2022a). Responses of groundwater and soil to dewatering considering the barrier effect of adjacent metro station on multi-aquifers. *Journal of Hydrology, 612*, 128117.
Zeng, C.-F., Powrie, W., Chen, H.-B., Wang, S., Diao, Y., & Xue, X.-L. (2024). Ground behavior due to dewatering inside a foundation pit considering the barrier effect of preexisting building piles on aquifer flow. *Journal of Geotechnical and Geoenvironmental Engineering, 150*(6), 05024004.
Zeng, C.-F., Song, W.-W., Xue, X.-L., Li, M.-K., Bai, N., & Mei, G.-X. (2021a). Construction dewatering in a metro station incorporating buttress retaining wall to limit ground settlement: insights from experimental modelling. *Tunnelling and Underground Space Technology, 116*, 104124.
Zeng, C.-F., Sun, H.-Y., Chen, H.-B., Xue, X.-L., Liu, Y.-S., & Song, W.-W. (2022). *Responses of Adjacent Building Pile to Foundation Pit Dewatering.* Paper presented at the Proceedings of the 4th International Conference on Performance Based Design in Earthquake Geotechnical Engineering, Cham.
Zeng, C.-F., Wang, S., Xue, X.-L., Zheng, G., & Mei, G.-X. (2021b). Evolution of deep ground settlement subject to groundwater drawdown during dewatering in a multi-layered aquifer-aquitard system: insights from numerical modelling. *Journal of Hydrology, 603*, 127078.
Zeng, C.-F., Wang, S., Xue, X.-L., Zheng, G., & Mei, G.-X. (2022c). Characteristics of ground settlement due to combined actions of groundwater drawdown and enclosure wall movement. *Acta Geotechnica, 17*, 4095–4112.
Zeng, C.-F., Xue, X.-L., & Li, M.-K. (2021c). Use of cross wall to restrict enclosure movement during dewatering inside a metro pit before soil excavation. *Tunnelling and Underground Space Technology, 112*, 103909.
Zeng, C.-F., Zheng, G., & Xue, X.-L. (2019a). Responses of deep soil layers to combined recharge in a leaky aquifer. *Engineering Geology, 260*, 105263.

Zeng, C.-F., Zheng, G., Zhou, X.-F., Xue, X.-L., & Zhou, H.-Z. (2019b). Behaviours of wall and soil during pre-excavation dewatering under different foundation pit widths. *Computers and Geotechnics, 115*, 103169.

Zeng, C. F., Powrie, W., Xue, X. L., Li, M. K., & Mei, G. X. (2021d). Effectiveness of a buttress wall in reducing retaining wall movement during dewatering before bulk excavation. *Acta Geotechnica, 16*, 3253–3267.

Zeng, C. F., Xue, X. L., Zheng, G., Xue, T. Y., & Mei, G. X. (2018). Responses of retaining wall and surrounding ground to pre-excavation dewatering in an alternated multi-aquifer-aquitard system. *Journal of Hydrology, 559*, 609–626.

Zeng, C. F., Zheng, G., Xue, X. L., & Mei, G. X. (2019c). Combined recharge: a method to prevent ground settlement induced by redevelopment of recharge wells. *Journal of Hydrology, 568*, 1–11.

Zhang, W., Wang, W., Zhou, D., Zhang, R., Goh, A. T. C., & Hou, Z. (2018a). Influence of groundwater drawdown on excavation responses – A case history in Bukit Timah granitic residual soils. *Journal of Rock Mechanics and Geotechnical Engineering, 10*(5), 856–864.

Zhang, W. G., Goh, A. T. C., Goh, K. H., Chew, O. Y. S., Zhou, D., & Zhang, R. (2018b). Performance of braced excavation in residual soil with groundwater drawdown. *Underground Space, 3*(2), 150–165.

Zhang, W. G., Li, H. R., Wu, C. Z., Li, Y. Q., Liu, Z. Q., & Liu, H. L. (2021). Soft computing approach for prediction of surface settlement induced by earth pressure balance shield tunneling. *Underground Space, 6*(4), 353–363.

Zheng, G., Ha, D., Loaiciga, H., Zhou, H., Zeng, C., & Zhang, H. (2019a). Estimation of the hydraulic parameters of leaky aquifers based on pumping tests and coupled simulation/optimization: verification using a layered aquifer in Tianjin, China. *Hydrogeology Journal, 27*(8), 3081–3095.

Zheng, G., Ha, D., Zeng, C., Cheng, X., Zhou, H., & Cao, J. (2019b). Influence of the opening timing of recharge wells on settlement caused by dewatering in excavations. *Journal of Hydrology, 573*, 534–545.

Zheng, G., Zeng, C. F., Diao, Y., & Xue, X. L. (2014). Test and numerical research on wall deflections induced by pre-excavation dewatering. *Computers and Geotechnics, 62*, 244–256.